Journal of Theoretical Biology 271 (2011) 114–123

Contents lists available at ScienceDirect

Journal of Theoretical Biology

journal homepage: www.elsevier.com/locate/yjtbi

The Bcl-2-associated death promoter (BAD) lowers the threshold at which the Bcl-2-interacting domain death agonist (BID) triggers mitochondria disintegration

Christopher C. Howells [a,*], William T. Baumann [a], David C. Samuels [b], Carla V. Finkielstein [c]

[a] Virginia Polytechnic Institute & State University, Department of Electrical & Computer Engineering, Blacksburg, VA 24061, USA
[b] Vanderbilt University Medical Center, Center for Human Genetics Research, Nashville, TN 37232, USA
[c] Integrated Cellular Responses Laboratory—Virginia Polytechnic Institute & State University, Department of Biological Sciences, Blacksburg, VA 24061, USA

ARTICLE INFO

Article history:
Received 6 June 2010
Received in revised form
3 November 2010
Accepted 24 November 2010
Available online 3 December 2010

Keywords:
Apoptosis
BAD
Bcl-2
Modeling
Bifurcation

ABSTRACT

The Bcl-2-associated death promoter (BAD) protein, like many other BH3-only proteins, is known to promote apoptosis through the intrinsic mitochondrial pathway. Unlike the BH3-interacting domain death agonist (BID) protein, BAD cannot directly trigger apoptosis but, instead, lowers the threshold at which apoptosis is induced. In many mathematical models of apoptosis, BAD is neglected or abstracted. The work presented here considers the incorporation of BAD and its various modifications in a model of the tBID-induction of BAK (Bcl-2 homologous antagonist killer) or the tBID-induction of BAX (Bcl-2-associated X protein). Steady state equations are used to develop an explicit formula describing the total concentration level of tBID, guaranteed to trigger apoptosis, as a bilinear function of the total BAD concentration level and the total anti-apoptotic protein concentration level (usually Bcl-2 or Bcl-x_L). In particular, the formula explains how the pro-apoptotic protein BAD lowers the threshold at which tBID induces BAK/BAX activation—reducing the level of total Bcl-2/Bcl-x_L available to inhibit tBID signaling in the mitochondria. Attention is then turned to the experimental data surrounding BAD phosphorylation, a process known to inhibit the pro-apoptotic effects of BAD. To address this data, the phosphorylation process is modeled following two separate kinetics in which either free unbound BAD is the assumed substrate or Bcl-x_L/Bcl-2-bound BAD is the assumed substrate. Bifurcation analysis and further analysis of the bilinear equation validate experiments, which suggest that BAD phosphorylation prevents irreversible BAK/BAX-mediated apoptosis, even when phosphorylation-induced dissociation of Bcl-x_L/Bcl-2-bound BAD is blocked. It is also shown that a cooperative, even synergistic, removal of mitochondrial BAD is seen when both types of phosphorylation are assumed possible. The presented work, however, reveals that the balance between BAD phosphorylation and dephosphorylation modulates the degree to which BAD influences the signaling from tBID to BAK/BAX. Our model shows that both the mode(s) of phosphorylation and the BAD dephosphorylation rate become important factors in determining whether BAD influences the activation of the BAK/BAX signal or not. Such potential variations in the pro-apoptotic effects of BAD are used to explain some of the inconsistent experimental data surrounding BAD phosphorylation. Nonetheless, our model serves to evaluate BAD and its sensitizing effects on the tBID-induction of BAK/BAX and thus aid in predicting when the incorporation of BAD in an apoptosis signaling model is important and when it is not.

1. Introduction

Apoptosis, or programmed cell death, is an essential process in all multi-cellular organisms. It is indispensable to an organism's development, adaptation, and maintenance. In particular, apoptosis prevents the propagation of malicious effects of damaged DNA caused, for example, by free radicals, radiation, and purine modifications, to daughter cells. Remarkably, many of the molecules involved in the intrinsic pathway cannot be definitively labeled as pro- or anti-apoptotic since many irregularities at the transcriptional and post-translational level influence these molecules' function (Shibasaki et al., 1997; Jambal et al., 2003; Shinoad et al., 2003). For example, Bcl-2, an otherwise anti-apoptotic protein, becomes inactive and no longer anti-apoptotic, when cleaved by caspase-3 (Won et al., 2002; Kim et al., 1998; Nicholson 1999).

The BH3-only-containing proteins BAD (**B**cl-2-**a**ssociated **d**eath promoter) and BID (**B**H3-**i**nteracting **d**omain death agonist) are molecules that possess a single region of homology with Bcl-2.

* Corresponding author. Tel.: +1 720 347 8375.
E-mail address: chowells@vt.edu (C.C. Howells).

0022-5193/$ - see front matter © 2010 Elsevier Ltd. All rights reserved.
doi:10.1016/j.jtbi.2010.11.040

BAD and BID can cause a healthy cell to become inappropriately apoptotic (Law et al., 2005; Yi et al., 2003; Berthier et al., 2004; Saito et al., 2003; Saito et al., 2000; Springer et al., 2000). In general, active BAD and BID trigger the oligomerizations of BAK (**B**cl-2 **a**ntagonistic **k**iller) and BAX (**B**cl-2-**a**ssociated **x** protein), which create pores and permeabilize the outer mitochondrial wall in a process known as mitochondrial outer membrane permeabilization (MOMP) (James and Green, 2004; Li et al., 1998; Wei et al., 2000; Saito et al., 2000). Sufficient permeabilization leads to the release of cytochrome-c and Smac from the mitochondria into the cytosol. In turn, these proteins remove the inhibition on effector caspases (such as caspase-3). Once un-inhibited, effectors caspases initiate the dismantling of the cell. As a result, MOMP is often viewed as the "point-of-no-return" for a cell.

Due to the complexity of the BH3-only protein interactions, as well as the potential therapeutic value that can be acquired through disentanglement, it becomes necessary to introduce mathematical models. Many models, including those that analyze the extrinsic pathway of apoptosis, have incorporated BID and its effect on downstream events (Chen et al., 2007; Hua et al., 2005; Bagci et al., 2006); BAD, on the other hand, has been neglected or limited to its behavior in the mitochondria (Chen et al., 2007).

What is generally missing from these models is a description of how pro-survival signals (often extending from outside the cell) lead to the partial or complete inactivation of BAD. In this paper, we propose a novel model that includes the phosphorylation (inactivation) of BAD, both inside and outside the mitochondria, alongside its Bcl-2-binding and Bcl-2-displacing capabilities in the mitochondria. Although much experimental data regarding the specifics associated with BAD phosphorylation is missing, an initial model can be developed and a qualitative assessment of the effects of BAD can be undertaken.

1.1. The BAD signaling pathway

BAD is considered active once it translocates to the mitochondria and becomes bound to Bcl-2 or Bcl-x_L as a heterodimer (Hekman et al., 2006; Adams and Cory 2007; Letai et al., 2002). In general, Bcl-2 and Bcl-x_L act in anti-apoptotic manners by binding pro-apoptotic proteins. Refer to Fig. 1. For example, binding the truncated form of BID (tBID), Bcl-2 and Bcl-x_L prevent tBID from inducing conformational changes in BAK and BAX, which lead to their activation (Wei et al., 2000; Wang et al., 1996; Cheng et al., 2001; Luo et al., 1998). Similarly, Bcl-2 and Bcl-x_L can bind BAK or BAX preventing their oligomerization (Letai et al., 2002; Oltvai et al., 1993; Sedlak et al., 1995; Yin et al., 1994; Valentijn et al., 2003; Gilmore et al., 2000). However, one exception to the rule is when Bcl-2 and Bcl-x_L bind BAD. In these cases, Bcl-2 and Bcl-x_L are only reducing their own usefulness since apoptotic signaling is more effectively inhibited when Bcl-2 and Bcl-x_L bind the more directly activating tBID, BAK, or BAX proteins. This is because BAD cannot *directly* activate tBID, BAK, or BAX. Taken from the perspective of BAD, this means that BAD acts in a pro-apoptotic fashion by binding Bcl-2 or Bcl-x_L, that is, reducing the level of anti-apoptotic proteins that safeguard from tBID signaling to BAK or

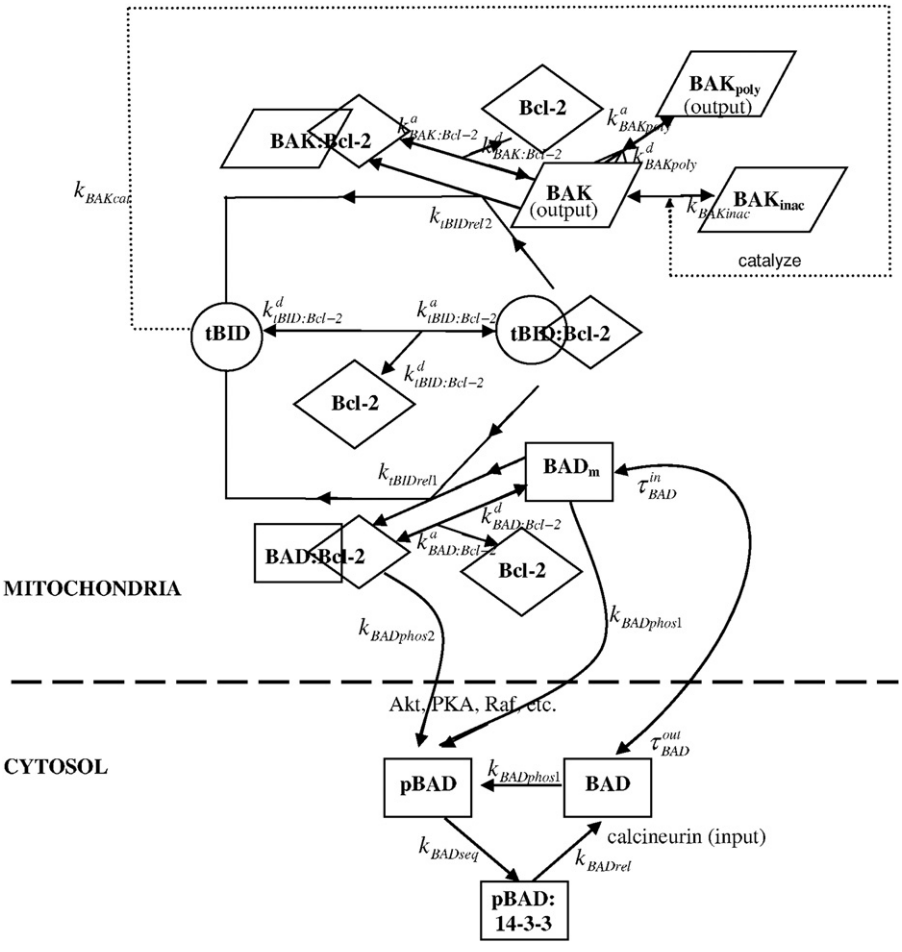

Fig. 1. BAD/tBID/BAK network. Post-translational network showing the reactions and states among BAD (rectangles), tBID (circles), BAK (parallelograms), and Bcl-2 (diamonds). The dotted arrow refers to the up-regulation of BAK via tBID. Curved arrows indicate re-localization processes between the cytoplasm and the mitochondria (lumped together as one big mitochondrion).

BAX. This is why BAD is often referred to as a *sensitizer* or an *enabler* (Chen et al., 2007; Hekman et al., 2006).

1.1.1. The phosphorylation of BAD

The BAD protein is inactivated through phosphorylation. The phosphorylation of BAD, and how growth and survival signals lead to its inactivation, has been given recent attention in the cellular biology literature, yet it remains to be clarified (Datta et al., 1997; Tan et al., 1999; Zhou et al., 2000; Peso et al., 1997; Zha et al., 1996; Wang et al., 1999). Below, we review the current knowledge of the phosphorylation of BAD keeping in mind that many of these findings are fragmented and sometimes contradictory.

Current research has established three critical sites of phosphorylation for BAD: Ser^{112}, Ser^{136}, and Ser^{155} (Datta et al., 1997; Tan et al., 1999; Zhou et al., 2000; Peso et al., 1997). Phosphorylation in Ser^{112} or Ser^{136} induces a conformational change in BAD such that a conserved binding site for the 14-3-3 protein, a molecular chaperone, is made available (Hekman et al., 2006; Zha et al., 1996; Wang et al., 1999). In such cases, 14-3-3 sequesters BAD on the cytoplasm, preventing BAD's interaction with Bcl-2 or Bcl-x_L. Kinases phosphorylate Ser^{155} BAD within its BH3 domain, blocking the ability of BAD to bind Bcl-2/Bcl-x_L. In this case, the chaperoning via 14-3-3 sequestration is unnecessary since BAD is already secured from activation regardless of whether BAD remains in the mitochondria or not (though 14-3-3 binding can still occur if BAD is further phosphorylated at Ser^{112} or Ser^{136}).

There are also phosphatases involved in controlling BAD availability. The most well-known is the Ca^{2+}-stimulated phosphatase calcineurin, which can dephosphorylate any of the above-mentioned phosphorylation sites (as well as remove 14-3-3 from BAD) (Berthier et al., 2004; Saito et al., 2003; Wang et al., 1999; Ayllon et al., 2000). If dephosphorylated (or left unphosphorylated), BAD can target the mitochondria or cytoplasm without any help from chaperoning molecules (Hekman et al., 2006).

Generally, phosphorylation of BAD occurs while BAD is in its free unbound form in the cytoplasm or the mitochondria; see Fig. 1. However, it is recently suggested that whenever BAD is bound to Bcl-x_L in the mitochondria, phosphorylation can induce the dissociation of the BAD:Bcl-x_L complex (Hekman et al., 2006; Datta et al., 1997; Zhou et al., 2000; Zha et al., 1996; Datta et al., 2000; Hirai and Wang, 2001). However, it is unclear the mechanism that mediates this process. The experiments in Zha et al. (1996) and Hirai and Wang (2001) illustrate the process as a simple consequence of Ser^{112} or Ser^{136} phosphorylation. On the other hand, experiments in Zhou et al. (2000) demonstrate that dissociation is still possible even when the Ser^{112} and Ser^{136} sites are replaced with unphosphorylatable alanine mutations. Conversely, experiments in Datta et al. (2000) and Hekman et al. (2006) suggest that Ser^{155} phosphorylation must follow Ser^{136} phosphorylation in order to trigger dissociation (though, oddly in other experiments in Datta et al. (2000), Ser^{155} phosphorylation is shown to work independently of Ser^{112} and Ser^{136} phosphorylations). Finally, at a completely different extreme, *in vitro* experiments in Strasser et al. (1997) show that Ser^{136} and Ser^{155} phosphorylations are not even possible when BAD is complexed with Bcl-x_L.

1.1.2. Mitochondrial outer membrane permeabilization

tBID directly induces the activation and subsequent oligomerization of BAK and BAX (e.g., into tetramers (Saito et al., 2000; Nechushtan et al., 2001)), forming pores through which lethal mitochondrially sequestered constituents are released into the cytosol (Li et al., 1998; Wei et al., 2000; Saito et al., 2000). In particular, the lethal constituent Smac removes the inhibition caused by XIAP, which normally keeps effector caspase-3 activity in check (Rehm et al., 2006). It is currently believed that once free BAK or BAX (unsequestered by Bcl-2) begins to accumulate in the mitochondria, a switch-like response is seen in the activity of caspase-3 (Albeck et al., 2008a, 2008b). Furthermore, whereas the time from signaling of certain death-inducing ligands to the initiation of this switch can vary – dependent upon BID concentration and its rate of processing into tBID (Spencer et al., 2009; Albeck et al., 2008a) – the time from the first formation of a pore to significant increased activity of caspase-3 is relatively static and extremely fast (Albeck et al., 2008b). In addition, these studies also show that concurrent blocking of MOMP and XIAP lead to a cell that is "half-dead", suggesting that the mitochondrial kinetics provide a certain degree of amplification. Such amplification in apoptotic signaling could of course be explained by a feedback loop. Several experimental and model-based studies have previously suggested feedback loops that extend outside the mitochondria (Bagci et al., 2006; Rehm et al., 2006; Aldridge et al., 2006), but recent work supports the switch-like mechanism as a consequence of mitochondrial kinetics only (Chen et al., 2007; Albeck et al., 2008b; Dussmann et al., 2010). In our effort to study the impact of the protein BAD, we will append the previously established tBID/BAX model from Chen et al. (2007) to our BAD model in order to see how BAD affects these switch-like and amplification properties.

2. Model and methods

2.1. Mathematical model of the BAD/tBID/BAK pathway

Since our focus is on the actions of BAD, we use the model structure and kinetic equations from Chen et al. (2007) for the states of tBID and BAK. Similar to the work done in Chen et al. (2007), "Bcl-2" is assumed to be a general term, which could denote Bcl-2 or Bcl-x_L. Similarly, "BAK" refers to BAK itself or translocated BAX.

To keep our model simple yet capable of addressing some of the issues discussed in Section 1.1.1, we modeled the overall phosphorylation of BAD with two kinetics: one for the phosphorylation of unbound BAD (which can occur either in the cytoplasm or mitochondria); and one for Bcl-2-bound BAD phosphorylation (which induces the dissociation of BAD from Bcl-2, see Fig. 1 or Table S1). We assume that these phosphorylations are irreversible in the sense that phosphorylated BAD (pBAD) must first bind 14-3-3 (to form pBAD:14-3-3) prior to any kind of dephosphorylation. This is consistent with the experimental data (Hekman et al., 2006), which demonstrate that once pBAD binds 14-3-3 (which they hypothesize to occur in the mitochondria and in the cytoplasm), the complex must first reach the plasma membrane before dissociation, and therefore dephosphorylation can occur. Even though 14-3-3 binding may not always be the reaction that immediately follows phosphorylation (as we said before, Ser^{155} phosphorylation may work independently of 14-3-3 chaperoning) our model does serve to illustrate how the sequestration of BAD provides a temporary removal (or prevention) of BAD activation in the mitochondria.

We model phosphorylation, dephosphorylation, 14-3-3 sequestration, and translocation of BAD with 1st-order kinetics. See Eqs. (1)–(5). The remaining processes associated with BAD, such as Bcl-2-heterodimerization and tBID-displacement, as well as the processes among the states of tBID and BAK, are modeled with the law of mass-action. Refer to Eqs. (1)–(12). These equations define the BAD/tBID/BAK model:

$$\frac{d}{dt}[\mathrm{BAD}] = k_{\mathrm{BAD\ rel}}[\mathrm{pBAD{:}14\text{-}3\text{-}3}] + \tau^{\mathrm{out}}_{\mathrm{BAD}}[\mathrm{BAD}_m] - (k_{\mathrm{BAD\ phos1}} + \tau^{\mathrm{in}}_{\mathrm{BAD}})[\mathrm{BAD}] \tag{1}$$

$$\frac{d}{dt}[\mathrm{pBAD}] = k_{\mathrm{BAD\ phos1}}[\mathrm{BAD}] + k_{\mathrm{BAD\ phos1}}[\mathrm{BAD}_m] + k_{\mathrm{BAD\ phos2}}[\mathrm{BAD:Bcl\text{-}2}] - k_{\mathrm{BAD\ seq}}[\mathrm{pBAD}] \tag{2}$$

$$\frac{d}{dt}[\text{pBAD:14-3-3}] = k_{\text{BAD seq}}[\text{pBAD}] - k_{\text{BAD rel}}[\text{pBAD:14-3-3}] \tag{3}$$

$$\begin{aligned}\frac{d}{dt}[\text{BAD}_m] = {} & \tau^{\text{in}}_{\text{BAD}}[\text{BAD}] + k^{d}_{\text{BAD:Bcl-2}}[\text{BAD:Bcl-2}] \\ & -(k_{\text{BAD phos1}} + \tau^{\text{out}}_{\text{BAD}})[\text{BAD}_m] - k^{a}_{\text{BAD:Bcl-2}}[\text{BAD}_m][\text{Bcl-2}] \\ & -k_{\text{tBID rel1}}[\text{BAD}_m][\text{tBID:Bcl-2}]\end{aligned} \tag{4}$$

$$\begin{aligned}\frac{d}{dt}[\text{BAD:Bcl-2}] = {} & k^{a}_{\text{BAD:Bcl-2}}[\text{BAD}_m][\text{Bcl-2}] \\ & + k_{\text{tBID rel1}}[\text{BAD}_m][\text{tBID:Bcl-2}] \\ & -(k_{\text{BAD phos2}} + k^{d}_{\text{BAD:Bcl-2}})[\text{BAD:Bcl-2}]\end{aligned} \tag{5}$$

$$\begin{aligned}\frac{d}{dt}[\text{tBID}] = {} & k^{d}_{\text{tBID:Bcl-2}}[\text{tBID:Bcl-2}] + k_{\text{tBID rel1}}[\text{BAD}_m][\text{tBID:Bcl-2}] \\ & + k_{\text{tBID rel2}}[\text{BAK}][\text{tBID:Bcl-2}] - k^{a}_{\text{tBID:Bcl-2}}[\text{tBID}][\text{Bcl-2}]\end{aligned} \tag{6}$$

$$\begin{aligned}\frac{d}{dt}[\text{tBID:Bcl-2}] = {} & k^{a}_{\text{tBID:Bcl-2}}[\text{tBID}][\text{Bcl-2}] - k^{d}_{\text{tBID:Bcl-2}}[\text{tBID:Bcl-2}] \\ & - k_{\text{tBID rel1}}[\text{BAD}_m][\text{tBID:Bcl-2}] \\ & - k_{\text{tBID rel2}}[\text{BAK}][\text{tBID:Bcl-2}]\end{aligned} \tag{7}$$

$$\begin{aligned}\frac{d}{dt}[\text{Bcl-2}] = {} & (k_{\text{BAD phos2}} + k^{d}_{\text{BAD:Bcl-2}})[\text{BAD:Bcl-2}] \\ & + k^{d}_{\text{tBID:Bcl-2}}[\text{tBID:Bcl-2}] + k^{d}_{\text{BAK:Bcl-2}}[\text{BAK:Bcl-2}] \\ & - k^{a}_{\text{BAD:Bcl-2}}[\text{BAD}_m][\text{Bcl-2}] - k^{a}_{\text{tBID:Bcl-2}}[\text{tBID}][\text{Bcl-2}] \\ & - k^{a}_{\text{BAK:Bcl-2}}[\text{BAK}][\text{Bcl-2}]\end{aligned} \tag{8}$$

$$\frac{d}{dt}[\text{BAK}_{\text{inac}}] = k_{\text{BAK inac}}[\text{BAK}] - k_{\text{BAK cat}}[\text{tBID}][\text{BAK}_{\text{inac}}] \tag{9}$$

$$\begin{aligned}\frac{d}{dt}[\text{BAK}] = {} & k_{\text{BAK cat}}[\text{tBID}][\text{BAK}_{\text{inac}}] + k^{d}_{\text{BAK:Bcl-2}}[\text{BAK:Bcl-2}] \\ & + 4k^{d}_{\text{BAK poly}}[\text{BAK}_{\text{poly}}] - k_{\text{BAK inac}}[\text{BAK}] \\ & - k^{a}_{\text{BAK:Bcl-2}}[\text{BAK}][\text{Bcl-2}] - k_{\text{tBID rel2}}[\text{BAK}][\text{tBID:Bcl-2}] \\ & - 4k^{a}_{\text{BAK poly}}[\text{BAK}]^4\end{aligned} \tag{10}$$

$$\frac{d}{dt}[\text{BAK:Bcl-2}] = k^{a}_{\text{BAK:Bcl-2}}[\text{BAK}][\text{Bcl-2}] + k_{\text{tBID rel2}}[\text{BAK}][\text{tBID:Bcl-2}] - k^{d}_{\text{BAK:Bcl-2}}[\text{BAK:Bcl-2}] \tag{11}$$

$$\frac{d}{dt}[\text{BAK}_{\text{poly}}] = k^{a}_{\text{BAK poly}}[\text{BAK}]^4 - k^{d}_{\text{BAK poly}}[\text{BAK}_{\text{poly}}] \tag{12}$$

In addition, total concentrations are defined as follows:

$$[\text{BAD}_{\text{total}}] = [\text{BAD}] + [\text{pBAD}] + [\text{pBAD:14-3-3}] + [\text{BAD}_m] + [\text{BAD:Bcl-2}] \tag{13}$$

$$[\text{tBID}_{\text{total}}] = [\text{tBID}] + [\text{tBID:Bcl-2}] \tag{14}$$

$$[\text{BAK}_{\text{total}}] = [\text{BAK}_{\text{inac}}] + [\text{BAK}] + [\text{BAK:Bcl-2}] + 4[\text{BAK}_{\text{poly}}] \tag{15}$$

$$[\text{Bcl-2}_{\text{total}}] = [\text{Bcl-2}] + [\text{BAD:Bcl-2}] + [\text{tBID:Bcl-2}] + [\text{BAK:Bcl-2}] \tag{16}$$

Note that Eqs. (1)–(12) imply the total concentrations of BAD, tBID, BAK, and Bcl-2, defined above, are fixed over time.

2.2. Specifying kinetic rate constant values

Although there is published experimental data concerning some of the kinetic parameters in Eqs. (1)–(12), most of these parameters are unknown or uncertain at best. However, as mentioned, we can make use of some of the values from previous models (Chen et al., 2007; Bagci et al., 2006), and for the remaining, we have estimated values from kinase and phosphatase assays, binding assays, and fluorescence polarization experiments. Table 1 summarizes these values alongside their references.

Table 1
Rate constant values used for the BAD/tBID/BAK model. $k_{\text{BAD phos1}}$ (unbound phosphorylation rate) and $k_{\text{BAD rel}}$ (dephosphorylation rate) are 1st-order estimations to the kinetic plots in Zhou et al. (2002) and Springer et al. (2000), respectively. The value of $k_{\text{BAD phos2}}$ (bound phosphorylation rate constant) is estimated to be an order of magnitude smaller than $k_{\text{BAD phos1}}$ to account for the delay brought on by unmodeled dynamics. Values of the Bcl-2 association rates for tBID and BAK, $k^{a}_{\text{tBID:Bcl-2}}$ and $k^{a}_{\text{BAK:Bcl-2}}$, respectively, are borrowed from Chen et al. (2007). It is assumed that bound Bcl-2 dissociates from BAD, tBID, or BAK at the same rate, .002 s^{-1} (close to the value used in Chen et al. (2007)). Association/dissociation rate constants also reflect a BAD/Bcl-x_L dissociation constant of less than 1 nM (Yaffe et al., 1997) and BAD's 5-times greater affinity for Bcl-2 than tBID's for Bcl-2 (Letai et al., 2002). The rate constant for tBID displacement, $k_{\text{tBID rel1}}$, is set to 33% of the association rate constant $k^{a}_{\text{BAD:Bcl-2}}$. $k^{d}_{\text{BAK poly}}$ is set small to reflect the irreversible nature in Chen et al. (2007), and then $k^{a}_{\text{BAK poly}}$ is adjusted accordingly to match (qualitatively) the bifurcation plots of $r_{\text{BAK}} = ([\text{BAK}] + 4[\text{BAK}_{\text{poly}}])/[\text{BAK}_{\text{total}}]$ and time response curves in Chen et al. (2007) for when there is no expression of BAD. The value of $k_{\text{BAD seq}}$ reflects the association rate constant between BAD and 14-3-3ζ isoform in Hekman et al. (2006) when 14-3-3ζ has a fixed concentration of 10 nM. Finally, the values of $\tau^{\text{in}}_{\text{BAD}}$ and $\tau^{\text{out}}_{\text{BAD}}$ are estimated to reflect the liposome-binding assay data in Hekman et al. (2006).

Rate constant	Value	Reference
$k_{\text{BAD phos1}}$	.001 s^{-1}	Obata et al. (2000), Zhou et al. (2002), Deprez et al. (1997)
$k_{\text{BAD phos2}}$	.0001 s^{-1}	Estimated
$k_{\text{BAD seq}}$	.001 s^{-1}	Hekman et al. (2006)
$k_{\text{BAD rel}}$	.00087 s^{-1}	Springer et al. (2000), Liu and Storm (1989), Wolff and Sved (1985)
$\tau^{\text{in}}_{\text{BAD}}$	.01 s^{-1}	Hekman et al. (2006)
$\tau^{\text{out}}_{\text{BAD}}$	.002 s^{-1}	Hekman et al. (2006)
$k^{a}_{\text{BAD:Bcl-2}}$	15 $\mu M^{-1} s^{-1}$	Letai et al. (2002)
$k^{d}_{\text{BAD:Bcl-2}}$	.002 s^{-1}	Estimated
$k^{a}_{\text{tBID:Bcl-2}}$	3 $\mu M^{-1} s^{-1}$	Chen et al. (2007)
$k^{d}_{\text{tBID:Bcl-2}}$	.002 s^{-1}	Estimated
$k_{\text{tBID rel1}}$	5 $\mu M^{-1} s^{-1}$	Letai et al. (2002)
$k_{\text{BAK cat}}$	.5 $\mu M^{-1} s^{-1}$	Chen et al. (2007)
$k_{\text{BAK inac}}$	.1 s^{-1}	Chen et al. (2007)
$k^{a}_{\text{BAK:Bcl-2}}$	2 $\mu M^{-1} s^{-1}$	Chen et al. (2007)
$k^{d}_{\text{BAK:Bcl-2}}$	.002 s^{-1}	Estimated
$k_{\text{tBID rel2}}$	2 $\mu M^{-1} s^{-1}$	Chen et al. (2007)
$k^{a}_{\text{BAK poly}}$	2000 $\mu M^{-3} s^{-1}$	Estimated
$k^{d}_{\text{BAK poly}}$	5E−5 s^{-1}	Estimated

2.3. Software used

Time simulations of the BAD/tBID/BAK model (Eqs. (1)–(12)) were carried out in MATLAB v6.5 using the integrator ode23.m. Bifurcation diagrams were generated using Oscill8 v2.0.9, which provides a graphical user interface to libraries based upon AUTO2000 (and can be downloaded for free at http://oscill8.sourceforge.net/).

3. Results

3.1. Simulation of the tBID-induction of BAK

Before we explain the sensitizing properties of BAD (Hekman et al., 2006; Letai et al., 2002; Kuwana et al., 2005; Goldsmith et al., 2006), we first observe how tBID is an activator of BAK. A positive feedback loop exists between tBID and BAK since active BAK can displace tBID from the tBID:Bcl-2 complex (as well as drive down the level of free Bcl-2) and tBID can activate BAK (see Fig. 1). Fig. 2a–d illustrates the time response behavior of Eqs. (1)–(12) for two different concentration levels of total tBID: one that is high enough to drive the activation of BAK (Fig. 2a and b) and another that is too low to do so (Fig. 2c and d). These simulations lead us to believe that only when free Bcl-2 is nearly exhausted do we witness tBID activating BAK, that is, do we see [BAK] > 0. Moreover, we only see the polymerization of BAK (indicated by [BAK_{poly}]) when Bcl-2 is nearly exhausted.

3.2. Bifurcation analyses reveal BAD as a sensitizer to the tBID-induction of BAK

Another way to observe the switch-like behavior between tBID and BAK is using bifurcation diagrams with [$tBID_{total}$] as the parameter. Fig. 3 is a bifurcation plot showing how steady state [BAK] varies with [$tBID_{total}$] for certain fixed levels of total [BAD_{total}]. For almost all levels of total BAD, our system exhibits bistability in a small interval between two saddle-node bifurcation points (with a maximum interval when there is no BAD), wherein two different stable steady state values of BAK can be obtained depending on where the system is initialized.

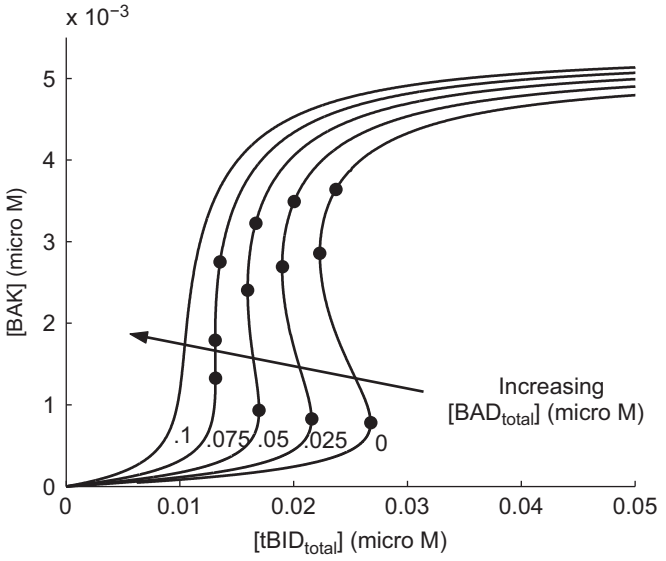

Fig. 3. BAD sensitizes the activation of BAK induced by tBID. One-parameter bifurcation diagram with total tBID as the bifurcation parameter for various fixed levels of total BAD. Here, we have set [$Bcl\text{-}2_{total}$] = 0.1 μ*M* and [BAK_{total}] = 0.2 μ*M*.

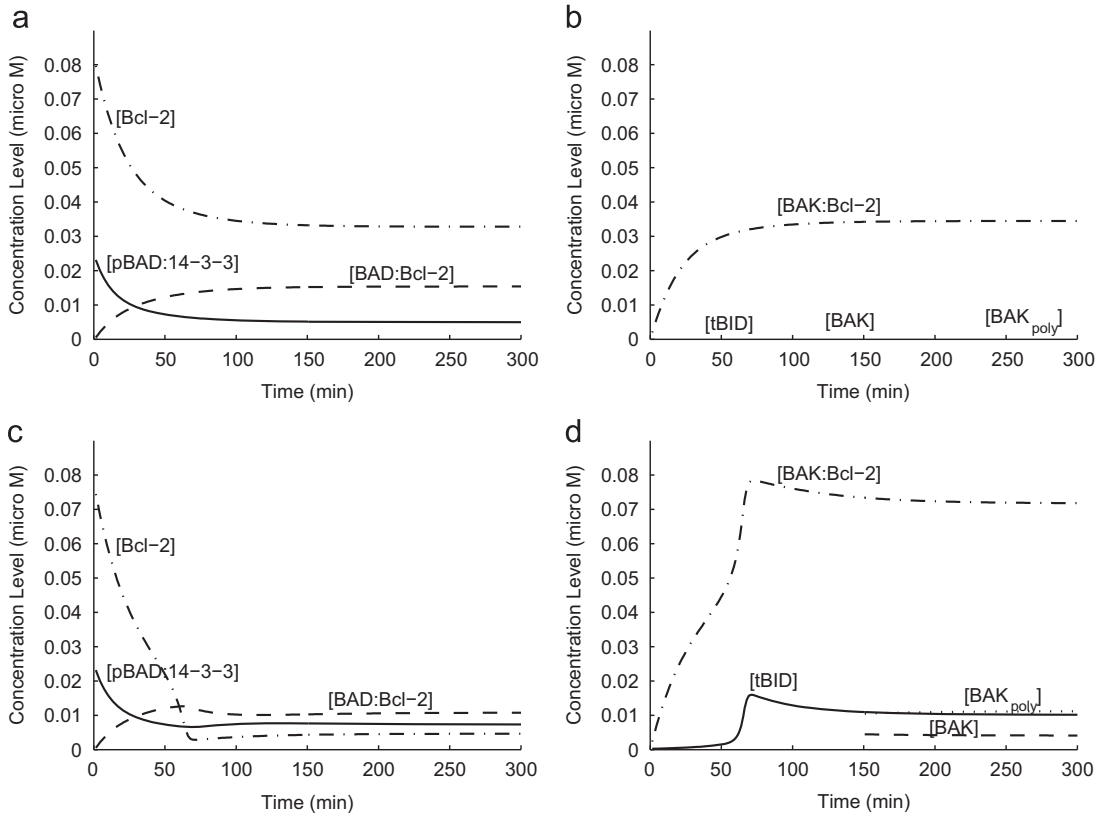

Fig. 2. Representative time response curves for two different levels of total tBID. (a)–(b) BAK inactivation when [$tBID_{total}$] = 0.018 μ*M* and; (c)–(d) BAK activation when [$tBID_{total}$] = 0.023 μ*M*. At time t=0, the following conditions have been assumed: [pBAD:14-3-3] = [BAD_{total}], [tBID:Bcl-2] = [$tBID_{total}$], [Bcl-2] = [$Bcl\text{-}2_{total}$]−[$tBID_{total}$], and [BAK_{inac}] = [BAK_{total}], where [BAD_{total}] = 0.025 μ*M*, [$Bcl\text{-}2_{total}$] = 0.1 μ*M*, and [BAK_{total}] = 0.2 μ*M*. All rate constants have been set to the values in Table 1.

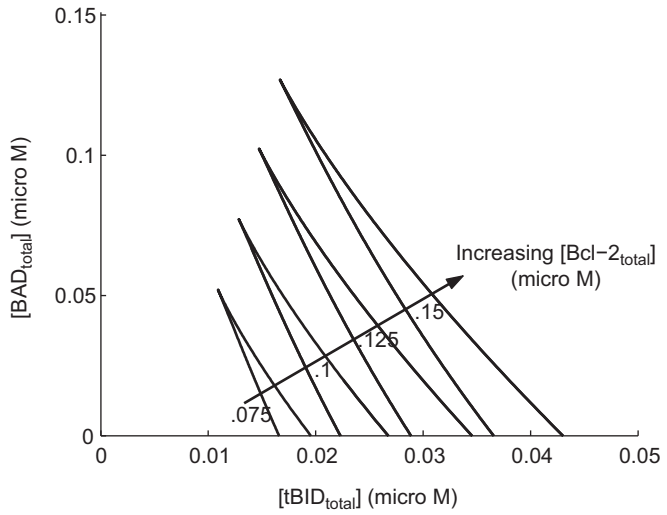

Fig. 4. BAD lowering the threshold mechanism between tBID and BAK. This 2-parameter diagram shows the evolution of both saddle-node bifurcation points as a function of total BAD for various fixed values of total Bcl-2. The rightmost line of each pair is the guaranteed triggering threshold for BAK activation.

For each level of total BAD, we take particular interest in the *rightmost* saddle-node bifurcation point since it represents the biologically meaningful threshold past which an initially inactive BAK is guaranteed to become active. That is, for any level of total tBID beyond this point, our system will move towards activation (Fig. 3), no matter what the initial condition is. We refer to this corresponding value of total tBID as the (total) tBID triggering level.

The 2-parameter bifurcation diagram in Fig. 4 illustrates how the tBID triggering level (rightmost line of each pair) evolves as a function of total BAD (and roughly as a function of total Bcl-2). Clearly, the tBID triggering level decreases in a nearly linear fashion as total BAD is increased. That is, an increase in total BAD corresponds to a proportional decrease in the total tBID triggering level. Clearly, BAD sensitizes the tBID-induction of BAK by lowering the threshold where tBID is guaranteed to activate BAK.

3.3. Simplifying the relationship among total BAD, total Bcl-2, and total tBID triggering levels

3.3.1. Explicit formula derivation

In Fig. 4, we see the relationship between total tBID and total BAD (as well as total Bcl-2) is approximately linear. At the coarsest level of approximation, we could assume that BAD in the mitochondria sequesters any available Bcl-2, bound or unbound. Any remaining Bcl-2 then binds to tBID preventing it from activating BAK. Only when [tBID$_{total}$] becomes greater than [Bcl-2$_{total}$]−[BAD$_{total}$] will there be free tBID, which can then activate BAK.

The high affinity of BAD for Bcl-2 (see Table 1) justifies the approximation that any BAD in the mitochondria binds Bcl-2, but the lower affinity of tBID for Bcl-2 requires a somewhat finer approximation to determine the amount of free tBID that triggers BAK activation.

Towards this end, consider the simple binding reaction between tBID and Bcl-2:

$$\text{tBID} + \text{Bcl-2} \leftrightarrow \text{tBID} : \text{Bcl-2} \tag{17}$$

If no other reactions are considered, the steady state level of free tBID can be computed as a function of the three parameters:

$$[\text{tBID}_{\text{total}}] = [\text{tBID}] + [\text{tBID:Bcl-2}]$$

$$[\text{Bcl-2}_{\text{total}}] = [\text{Bcl-2}] + [\text{tBID:Bcl-2}]$$

$$K_{D\ \text{tBID}} = k^d_{\text{tBID:Bcl-2}} / k^a_{\text{tBID:Bcl-2}}$$

the last parameter being the dissociation constant. From (17) we have that the steady state level of free tBID satisfies the quadratic equation:

$$[\text{tBID}]^2 + (K_{D\ \text{tBID}} + [\text{Bcl-2}_{\text{total}}] - [\text{tBID}_{\text{total}}])[\text{tBID}] - K_{D\ \text{tBID}}[\text{tBID}_{\text{total}}] = 0 \tag{18}$$

Eq. (18) has only one positive root, which is the unique steady state level of free tBID. Setting the level of free tBID to the level required for BAK activation, [tBID$_{act}$], which we will assume to be a constant, we can solve for the level of total tBID necessary to trigger the activation of BAK:

$$[\text{tBID}_{\text{total}}] = [\text{tBID}_{\text{act}}] + \frac{[\text{tBID}_{\text{act}}]}{K_{D\ \text{tBID}} + [\text{tBID}_{\text{act}}]} [\text{Bcl-2}_{\text{total}}] \tag{19}$$

To account for the fact that total available Bcl-2 is reduced by the amount of BAD in the mitochondria we replace [Bcl-2$_{total}$] with [Bcl-2$_{total}$]−$r_{\text{BAD:Bcl-2}}$[BAD$_{total}$], resulting in

$$[\text{tBID}_{\text{total}}] = [\text{tBID}_{\text{act}}] + \frac{[\text{tBID}_{\text{act}}]}{K_{D\ \text{tBID}} + [\text{tBID}_{\text{act}}]} ([\text{Bcl-2}_{\text{total}}] - r_{\text{BAD:Bcl-2}}[\text{BAD}_{\text{total}}]) \tag{20}$$

The coefficient $r_{\text{BAD:Bcl-2}}$ accounts for the fact that not all BAD may reside in the mitochondria, but rather some may remain in the cytosol. Using Eqs. (1)–(5) we can write

$$r_{\text{BAD:Bcl-2}} = \frac{[\text{BAD:Bcl-2}]}{[\text{BAD}_{\text{total}}]} = \frac{1}{1 + \alpha_2 + (1+\alpha_1)\beta_2 + (1+\alpha_1)(1+\beta_1)\gamma} \tag{21}$$

where

$$\alpha_1 = \frac{k_{\text{BAD phos1}}}{k_{\text{BAD seq}}} + \frac{k_{\text{BAD phos1}}}{k_{\text{BAD rel}}}$$

$$\alpha_2 = \frac{k_{\text{BAD phos2}}}{k_{\text{BAD seq}}} + \frac{k_{\text{BAD phos2}}}{k_{\text{BAD rel}}}$$

$$\beta_1 = \frac{k_{\text{BADphos1}} + \tau^{\text{out}}_{\text{BAD}}}{\tau^{\text{in}}_{\text{BAD}}}$$

$$\beta_2 = \frac{k_{\text{BAD phos2}}}{\tau^{\text{in}}_{\text{BAD}}}$$

and where

$$\gamma = \frac{k_{\text{BAD phos2}} + k^d_{\text{BAD:Bcl-2}}}{k^a_{\text{BAD:Bcl-2}}[\text{Bcl-2}] + k_{\text{tBID rel1}}[\text{tBID:Bcl-2}]}$$

The assumption that γ is small is reasonable when the level of total tBID has yet to *surpass* the triggering level. This is because we do not expect to see much free tBID until this occurs, making [tBID:Bcl-2] relatively large. Consequently, we make the approximation that

$$r_{\text{BAD:Bcl-2}} = \frac{1}{1 + \alpha_2 + (1+\alpha_1)\beta_2}$$

Finally, substituting this value of $r_{\text{BAD:Bcl-2}}$ back into Eq. (20), we arrive to our approximation for the tBID triggering levels:

$$[\text{tBID}_{\text{total}}] = [\text{tBID}_{\text{act}}] + \frac{[\text{tBID}_{\text{act}}]}{K_{D\ \text{tBID}} + [\text{tBID}_{\text{act}}]} [\text{Bcl-2}_{\text{total}}] - \frac{[\text{tBID}_{\text{act}}]}{K_{D\ \text{tBID}} + [\text{tBID}_{\text{act}}]} \frac{1}{1 + \alpha_2 + (1+\alpha_1)\beta_2} [\text{BAD}_{\text{total}}] \tag{22}$$

Towards our interest in the role of phosphorylation (which will be pursued in more detail in subsequent sections), we see that

$r_{BAD:Bcl\text{-}2}$ in Eq. (21), indicating the degree of BAD activation, is directly dependent on the ratio of $k_{BAD\ phos2}$ (the bound form of phosphorylation) to $k_{BAD\ seq}$ (14-3-3-sequestration), to $k_{BAD\ rel}$ (dephosphorylation), and to τ^{in}_{BAD} (translocation). $r_{BAD:Bcl\text{-}2}$ is also dependent on the ratio of $k_{BAD\ phos1}$ (the unbound form of phosphorylation) to $k_{BAD\ seq}$, and to $k_{BAD\ rel}$ only through the product with the ratio of $k_{BAD\ phos2}$ to τ^{in}_{BAD}. Therefore, whereas phosphorylation associated with the bound form of BAD is independently effective towards the removal of BAD from the mitochondria, phosphorylation associated with the unbound form seems to require cooperation from the other form of phosphorylation or a reduction in translocation.

3.3.2. Numerical example

To check the accuracy of our approximation in Eq. (22) alongside the bifurcation diagram in Fig. 4, we first need to compute the coefficients for $[Bcl\text{-}2_{total}]$ and $[BAD_{total}]$. Using one of the x-intercepts in Fig. 4 (e.g., $[tBID_{total}] = .0267\ \mu M$ and $[Bcl\text{-}2_{total}] = .1\ \mu M$) we can use Eq. (18) to solve for $[tBID_{act}]$, which in this case gives $[tBID_{act}] = 2.4 \times 10^{-4}\ \mu M$. Other x-intercepts in Fig. 4 produce similar results. With the set of rate constants in Table 1 we can compute $K_{D\ tBID}$, α_1, α_2, and β_2. Finally, substituting all values into Eq. (22), we arrive to our approximation of the tBID triggering levels in Fig. 4:

$$[tBID_{total}] = 2.4 \times 10^{-4}\ \mu M + 0.26[Bcl\text{-}2_{total}] - 0.18[BAD_{total}] \quad (23)$$

We first take note of the coefficient 0.26. According to Eq. (22), this coefficient is dependent on the values of the dissociation constant $K_{D\ tBID}$ and the free triggering level $[tBID_{act}]$ and can range anywhere from zero to unity. The stronger the affinity between tBID and Bcl-2, the larger the coefficient and the greater the amount of tBID needed to induce triggering. In particular, a coefficient of unity implies that the total tBID must reach the same total level of Bcl-2 before triggering is guaranteed to occur. In our case, the coefficient of 0.26 means that tBID must reach approximately a quarter of total Bcl-2 to ensure that BAK is triggered.

According to Eq. (22), the magnitude of the second coefficient is the same as the first coefficient multiplied by the factor $r_{BAD:Bcl\text{-}2}$, which, in our case, means approximately 70% of the total BAD makes it into the mitochondria. Note that if all BAD were to make it into the mitochondria, then we would expect to see the second coefficient be the negative of the first coefficient.

3.3.3. Comparing approximation and Fig. 4

We superimpose our linear approximations predicted by Eq. (23) (shown in red) onto Fig. 4. The results are shown in Fig. 5. Note that each red line approximates the evolution of the rightmost saddle-node (or tBID triggering level) for some fixed level of total Bcl-2. Our approximation is accurate unless total BAD is small *and* total Bcl-2 is large. In these cases, guaranteed triggering actually occurs for larger levels of total tBID than what is predicted by our approximation. That is, with limited amounts of BAD, a surplus of Bcl-2 can more easily target BAK upon its attempted activation. This inhibits BAK activation and consequently necessitates a slightly larger level of tBID to overcome. Of course, the modeling of BAK was not factored into our approximation. Such a situation illustrates, however, yet another reason why Bcl-2 overexpression is a detrimental (and pathological) deregulator of appropriate apoptotic responses (Fahy et al., 2005).

Our approximation demonstrates two important facts of the BAD/tBID/BAK network: first, the impact of BAD on the tBID-induction of BAK is much like a titration process where the activation of BAD reflects the amount of Bcl-2 that is sequestered away from tBID; and second, the level of BAD activation, given as the ratio of Bcl-2-bound BAD to total BAD, is a function of rate constants only.

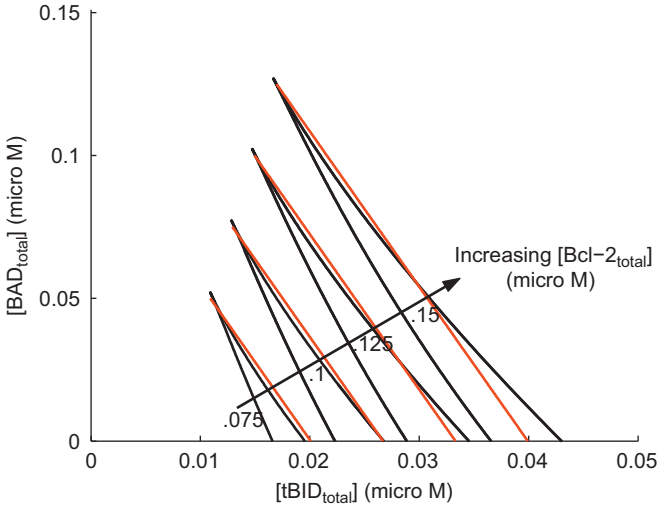

Fig. 5. Approximation (Eq. (23)) to the rightmost saddle-nodes in Fig. 4 (shown in red). (For interpretation of the references to colour in this figure legend, the reader is referred to the web version of this article.)

3.4. Comparison of model behavior to experimental data

We consider studies that have analyzed the impact of various synthetic peptides derived from the BH3 domains of BAD and BID (usually labeled BADBH3 and BIDBH3, respectively). In many of these studies, peptides are injected into cells or isolated mitochondria and compared according to how effective they are in inducing apoptosis. Then, the results are used to hypothesize the behaviors of the endogenous counterparts.

These studies demonstrate three basic facts about BAD and tBID. First, BAD is incapable of triggering apoptosis by itself (Letai et al., 2002; Kuwana et al., 2005; Goldsmith et al., 2006). Second, the presence of both peptides is shown to behave synergistically, affecting cells more than would be predicted through additive stoichiometry (Goldsmith et al., 2006; Kuwana et al., 2005). Stated another way, these two findings indicate that BAD can only lower the threshold at which tBID can activate BAK. And third, without some form of Bcl-2-like expression (e.g., Bcl-2, Mcl-1, or Bcl-x_L), this synergy between BAD and BID is absent (Letai et al., 2002; Kuwana et al., 2005).

The first and third facts are simple consequences of the network structure itself (Fig. 1), since the primary activity of BAD is to displace Bcl-2 and not directly activate tBID or BAK. Indeed, the absence of tBID or Bcl-2 would preclude the activation of BAD having any impact on this network. The synergy recognized between BAD and tBID is easily seen in Fig. 4. At any point on the lines in Fig. 4 such that total BAD is non-zero, the levels of BAD and tBID by themselves are incapable of triggering activation, whereas together they are capable of triggering activation.

3.5. The role of phosphorylation

The phosphorylation and dephosphorylation processes determine the proportion of BAD that is available to displace Bcl-2, and hence modulate the degree of sensitization of tBID-induction of BAK. Phosphatases like calcineurin drive the activation of BAD through the release of BAD from sequestration while kinases inhibit this activation through phosphorylation (Fig. 1).

In order to address how phosphorylation and dephosphorylation affect the activation of BAK, 2-parameter bifurcation diagrams are once again generated but, in this instance, we use the phosphorylation and dephosphorylation rates as parameters (more specifically, the kinetic rate constants). Furthermore, two

specific cases will be considered: one where the phosphorylation rate associated with the bound form of BAD (that is, $k_{\text{BAD phos2}}$) is non-zero; and another where $k_{\text{BAD phos2}}$ is zero. The first case is motivated by the experimental data in Yang et al. (1995), Zha et al. (1996) and Hirai and Wang (2001), which show that the extracellular survival factor, interleukin-3 (IL-3), can stimulate the phosphorylation-induced dissociation of BAD:Bcl-x_L in Bcl-x_L-expressing FL5.12 cells. We analyze such behavior within our model using a single phosphorylation parameter, $k_{\text{BAD phos}}$, where

$$k_{\text{BAD phos}} = k_{\text{BAD phos1}} = 100k_{\text{BAD phos2}},$$

as one of our bifurcation parameters. The remaining parameter is chosen to be $k_{\text{BAD rel}}$, reflecting the dephosphorylation rate. The results of the bifurcation analysis are shown in Fig. 6. Like Fig. 4, Fig. 6 shows bistability and a threshold mechanism. In general, sufficiently low phosphorylation rates ($k_{\text{BAD phos}} < .01\,\text{s}^{-1}$) are seen to activate BAK (brought on, of course, by the accumulation of mitochondrial BAD), and sufficiently high phosphorylation rates ($k_{\text{BAD phos}} > .05\,\text{s}^{-1}$) are necessary to keep BAK inactivated. The former is consistent with some studies that have shown that growth-factor-withdrawal can cause cells to become apoptotic merely from *lack* of BAD phosphorylation (Yang et al., 1995; Datta et al., 1997; Tan et al., 1999; Zha et al., 1996; Wang et al., 1999; Hirai and Wang, 2001). The latter is consistent with the studies that show that the pathological up-regulation of BAD phosphorylation can lead to the survival and proliferation of several types of pre-cancerous and cancerous cells (Dillon et al., 2007; Peso et al., 1997; Claerhout et al., 2007; Nicholson and Anderson, 2002).

Of particular interest in Fig. 6 are the saddle-node lines partitioning the bistable and monostable regions. They are relatively vertical for dephosphorylation rates above 0.005 s^{-1} (recall that our previous simulations were operating near $k_{\text{BAD rel}} = .001\,\text{s}^{-1}$). This means that for certain phosphorylation rates, no matter how strongly we drive the release of BAD through dephosphorylation, we can never activate BAK. In other words, there is a certain maximum impact that dephosphorylation can impart to this system. Inspection of Fig. 1 reveals that because we modeled the phosphorylation and sequestration processes of BAD such that BAD must be sequestered by 14-3-3 prior to dephosphorylation, 14-3-3 sequestration becomes a rate-limiting step to dephosphorylation. In particular, because we used $k_{\text{BAD seq}} = .001\,\text{s}^{-1}$ in generating this bifurcation diagram, it is clear that dephosphorylation loses its incremental effectiveness at approximately 5 times the sequestration rate.

There is also a large amount of experimental data that would suggest the absence of phosphorylation-induced dissociation of the BAD complex. For example, Hirai and Wang (2001) show that IL-3-stimulated Bcl-2-expressing FL5.12 cells are incapable of dissociating the BAD:Bcl-2 complex (where, in this case, Bcl-2 denotes the actual protein and not a family of proteins). Datta et al. (2000) also indicate that if it is necessary that Ser^{136} and Ser^{155} phosphorylation work concomitantly in order to dissociate the BAD complex (Datta et al., 2000), then any survival signals relying solely on stimulation via Akt, predominantly a Ser^{136} kinase, would be limited to the unbound form of phosphorylation only.

We can use our model to address this situation assuming

$$k_{\text{BAD phos}} = k_{\text{BADphos1}}, \quad k_{\text{BAD phos2}} = 0$$

Producing bifurcation plots for this second case (Fig. 7) much like we did for the previous case, we see the plot shifting to the right. This means that a generally higher demand upon the phosphorylation rate is required to prevent triggering. Nonetheless, sufficient phosphorylation is still capable of inhibiting dephosphorylation signaling of BAD despite the absence of the capacity for phosphorylation-induced BAD:Bcl-2 dissociation. This could explain why in some cells, certain kinases (such as Akt), without any evidence of inducing dissociation, can still inhibit the activation of BAD and apoptosis (Datta et al., 1997; Tan et al., 1999; Zhou et al., 2000; Peso et al., 1997; Wang et al., 1999; Claerhout et al., 2007).

Because of the shifting to the right, we can say the dephosphorylation rate becomes more effective in triggering BAK. That is, there exist more phosphorylation rates where dephosphorylation could still potentially trigger BAK. Conversely, given a certain dephosphorylation rate, the demand upon phosphorylation for guaranteed cell viability has increased approximately two-fold. Since kinase levels may vary from experiment to experiment, this may explain why Akt works as an inhibitor in one case but fails to do so in another. That is, unlike the experiments just mentioned in which Akt restores cell viability, Datta et al. (2000) argue in their mutation experiments that Akt restoration of cell viability when phosphorylation-induced dissociation of BAD:Bcl-x_L is blocked is impossible.

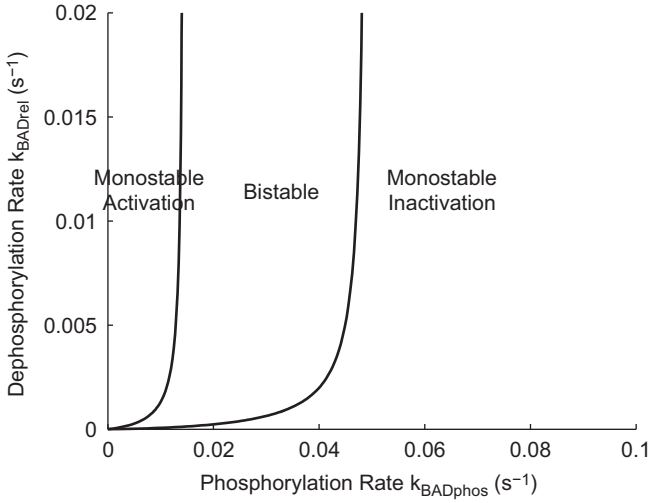

Fig. 6. Effect of simultaneous unbound and bound forms of phosphorylation on the bistability of BAK activation. Here, we have set $[\text{BAD}_{\text{total}}] = 0.05\,\mu M$, $[\text{Bcl-2}_{\text{total}}] = 0.1\,\mu M$, $[\text{BAK}_{\text{total}}] = 0.2\,\mu M$, and $[\text{tBID}_{\text{total}}] = 0.015\,\mu M$ (chosen close to a triggering point). Other rate constants have been set to the values in Table 1.

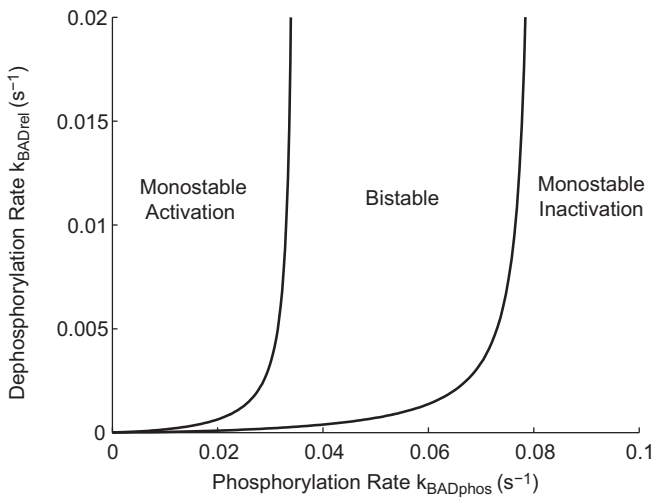

Fig. 7. Increased demand upon phosphorylation rates when phosphorylation-induced dissociation of BAD:Bcl-2 is no longer possible. Here, we have set $[\text{BAD}_{\text{total}}] = 0.05\,\mu M$, $[\text{Bcl-2}_{\text{total}}] = 0.1\,\mu M$, $[\text{BAK}_{\text{total}}] = 0.2\,\mu M$, and $[\text{tBID}_{\text{total}}] = 0.015\,\mu M$ (chosen close to a triggering point). Other rate constants have been set to the values in Table 1.

4. Discussion

BAD acts as a sensitizer by displacing Bcl-2 from tBID. This lowers the threshold amount of tBID needed to induce the activation of BAK. In a sense, the addition of BAD can be thought of as a titration system, in which BAD molecules pick off Bcl-2 molecules one-by-one until activation of BAK occurs. In some instances, the levels of BAD and tBID by themselves are insufficient to trigger BAK, but together they are capable of triggering activation. This means that BAD can have a profound effect on whether a cell becomes apoptotic or not. It is also thought that the delay prior to MOMP plays a role in whether a cell becomes apoptotic or not since, for example, a sufficient delay could give a cell enough time to counteract apoptotic signaling with alternate pro-survival pathways (Albeck et al., 2008b). Increased delay in our model could be caused by a decreased level of BAD or an increased level of free Bcl-2, which would require more processing of BID in order to reach the triggering level. Although we did not investigate transient properties of the network, such a reduction in BAD might be accomplished transiently through the phosphorylation of BAD.

In our modeling of the MOMP transition, we followed the approach in Chen et al. (2007), which results in a bistable system for BAK expression and allows for the large, fast release of Smac and cytochrome-c from the mitochondria, as is observed experimentally. But bistability is not necessary to create this quick release behavior, as is shown quite persuasively in the recent work modeling the extrinsic apoptotic pathway (Spencer et al., 2009; Albeck et al., 2008a, 2008b). Although these models eliminate positive feedback in the mitochondrial reactions, and hence bistability, they still produce what the authors term "snap-action" behavior in the release of Smac and cytochrome-c, and the subsequent activation of the downstream effector caspases. The snap-action behavior in their models is due to a very tight control on pore formation – essentially no pores are formed until seconds before the release due to MOMP occurs – and the sharp concentration gradient that allows a relatively small number of pores to transport a large quantity of Smac and cytochrome-c in a short period of time. The fact that the release due to MOMP occurs shortly after pores initially begin to form was validated experimentally in Albeck et al. (2008b) and also by the recent work in Dussmann et al. (2010). This latter work also used a cellular automaton modeling approach to demonstrate that pores can form quickly even with a minimal amount of active BAX, validating one aspect of the model results in Albeck et al. (2008b) using an alternative approach.

Although in this paper we have used bistability to achieve the experimentally observed snap-action release due to MOMP, our results with respect to BAD do not depend on bistability. While bistability of BAK as a function of tBID occurs in our model within a subset of the parameter space, weaker affinities between Bcl-2 and the three pro-apoptotic proteins (BAD, tBID, or BAK) in our model suffice to entirely remove the bistable region (similarly in the case of Chen et al.'s (2007) BAX activation module). In our analysis, the affinities of tBID/Bcl-2 and BAK/Bcl-2 were set relative to a rather tight BAD/Bcl-x_L affinity, which was less than 1 nM (Yaffe et al., 1997); however, there is experimental data that supports binding affinities looser by up to two orders of magnitude (Hua et al., 2005; Letai et al., 2002). Moreover, removal of the positive feedback loop (BAK displacing tBID from Bcl-2) in order to partially emulate the mathematical model in Albeck et al. (2008b) does not generate bistability. Remarkably, despite the disappearance of the bistable region due to parameter variation or network changes, the highly sigmoidal behavior from an initially inactive BAK to an active BAK induced by tBID remains, and the sensitization due to BAD remains as well. Hence, our results remain qualitatively correct even in the absence of a bistable model.

An important question to ask is whether the bifurcation plots (Figs. 3 and 4) tell us everything we need to know about the dynamical behavior of this network. From a nonlinear systems perspective, making general statements about the behavior of the BAD/tBID/BAK model, based upon specific rate constants, would be insufficient. Our bifurcation diagrams cannot, for example, preclude the existence of nonlinear behaviors such as periodic orbits. On the other hand, BAD/tBID/BAK is a conservative system, where total BAD, tBID, BAK, and Bcl-2 are constant for all time. Moreover, the presence of Bcl-2 and the high-order kinetics of BAK with an essentially zero dissociation rate make the behavior of this network tend towards inactivation or activation of BAK and remain there in a robust manner.

Appendix A. Supporting information

Supplementary data associated with this article can be found in the online version at doi:10.1016/j.jtbi.2010.11.040.

References

Adams, J.M., Cory, S., 2007. The Bcl-2 apoptotic switch in cancer development and therapy. Oncogene 26, 1324–1337.

Ayllon, V., Martinez-A, C., Garcia, A., Cayla, X., Rebollo, A., 2000. Protein phosphatase 1α is a Ras-activated Bad phosphatase that regulates interleukin-2 deprivation-induced apoptosis. EMBO Journal 19 (10), 2237–2246.

Albeck, J.G., Burke, J.M., Aldridge, B.B., Zhang, M., Lauffenburger, D.A., Sorger, P.K., 2008a. Quantitative analysis of pathways controlling extrinsic apoptosis in single cells. Molecular Cell 30, 11–25.

Albeck, J.G., Burke, J.M., Spencer, S.L., Lauffenburger, D.A., Sorger, P.K., 2008b. Modeling a snap-action, variable-delay switch controlling extrinsic cell death. PLoS Biology 6 (12), 2831–2852.

Aldridge, B.B., Haller, G., Sorger, P.K., Lauffenburger, D.A., 2006. Direct Lyapunov exponent analysis enables parametric study of transient signaling governing cell behaviour. IEE Proceedings—Systems Biology 153 (6), 425–432.

Berthier, A., Lemaire-Ewing, S., Prunet, C., Monier, S., Athias, A., Bessede, G., Barros, J.-P.P.d., Laubriet, A., Gambert, P., Lizard, G., Neel, D., 2004. Involvement of a calcium-dependent dephosphorylation of Bad associated with the localization of Trpc-1 within lipid rafts in 7-ketocholesterol-induced THP-1 cell apoptosis. Cell Death and Differentiation 11, 897–905.

Bagci, E.Z., Vodovotz, Y., Billiar, T.R., Ermentrout, G.B., Bahar, I., 2006. Bistability in apoptosis: roles of Bax, Bcl-2, and mitochondrial permeability transition pores. Biophysical Journal 90, 1546–1559.

Chen, C., Cui, J., Lu, H., Wang, R., Zhang, S., Shen, P., 2007. Modeling of the role of a Bax-activation switch in the mitochondrial apoptosis decision. Biophysical Journal 92, 4304–4315.

Cheng, E.H.-Y.A., Wei, M.C., Weiler, S., Flavell, R.A., Mak, T.W., Lindsten, T., Korsmeyer, S.J., 2001. BCL-2 BCL-XL sequesters BH3 domain-only molecules preventing BAX- and BAK-mediated mitochondrial apoptosis. Molecular Cell 8, 705–711.

Claerhout, S., Decraene, D., Laethem, A.V., Kelst, S.V., Agostinis, P., Garmyn, M., 2007. AKT delays the early-activated apoptotic pathway in UVB-irradiated keratinocytes via BAD translocation. Journal of Investigative Dermatology 127, 429–438.

Dillon, R.L., White, D.E., Muller, W.J., 2007. The phosphatidyl inositol 3-kinase signaling network: implications for human breast cancer. Oncogene 26, 1338–1345.

Datta, S.R., Dudek, H., Tao, X., Masters, S., Fu, H., Gotoh, Y., Greenberg, M.E., 1997. Akt phosphorylation of BAD couples survival signals to the cell-intrinsic death machinery. Cell 91, 231–241.

Datta, S.R., Katsov, A., Hu, L., Petros, A., Fesik, S.W., Yaffe, M.B., Greenberg, M.E., 2000. 14-3-3 proteinds and survival kinases cooperate to inactivate BAD by BH3 domain phosphorylation. Molecular Cell 6, 41–51.

Deprez, J., Vertommen, D., Alessi, D.R., Hue, L., Rider, M.H., 1997. Phosphorylation and activation of heart 6-phosphofructo-2-kinase by protein kinase B and other protein kinases of the insulin signaling cascade. Journal of Biological Chemistry 272 (28), 17269–17275.

Dussmann, H., Rehm, M., Concannon, C.G., Anguissola, S., Wurstle, M., Kacmar, S., Voller, P., Huber, H.J., Prehn, J.H.M., 2010. Single-cell quantification of Bax activation and mathematical modelling suggest pore formation on minimal mitochondrial Bax accumulation. Cell Death and Differentiation 17, 278–290.

Fahy, B.N., Schlieman, M.G., Mortenson, M.M., Virudachalam, S., Bold, R.J., 2005. Targeting BCL-2 overexpression in various human malignancies through NF-κB inhibition by the proteasome inhibitor bortezomib. Cancer Chemotherapy and Pharmocology 56, 46–54.

Goldsmith, K.C., Liu, X., Dam, V., Morgan, B.T., Shabbout, M., Cnaan, A., Letai, A., Korsmeyer, S.J., Hogarty, M.D., 2006. BH3 peptidomimetics potently activate apoptosis and demonstrate single agent efficacy in neuroblastoma. Oncogene 25, 4525–4533.

Gilmore, A.P., Metcalfe, A.D., Romer, L.H., Streuli, C.H., 2000. Integrin-mediated survial signals regulate the apoptotic function of Bax through its conformation and subcellular localization. Journal of Cell Biology 149, 431–445.

Hua, F., Cornejo, M.G., Cardone, M.H., Stokes, C.L., Lauffenburger, D.A., 2005. Effects of Bcl-2 levels on Fas signaling-induced caspase-3 activation: molecular genetic tests on computational model predictions. Journal of Immunology 175, 985–995.

Hekman, M., Albert, S., Galmiche, A., Rennefahrt, U.E.E., Fueller, J., Fischer, A., Puehringer, D., Wiese, S., Rapp, U.R., 2006. Reversible membrane interaction of BAD requires two C-terminal lipid binding domains in conjunction with 14-3-3 protein binding. Journal of Biological Chemistry 281 (25), 17321–17336.

Hirai, I., Wang, H.-G., 2001. Survival-factor-induced phosphorylation of Bad results in its dissociation from Bcl-xL but not Bcl-2. Biochemical J. 359, 345–352.

Jambal, P., Masterson, S., Nesterova, A., Bouchard, R., Bergman, B., Hutton, J.C., Boxer, L.M., Reusch, J.E.-B., Pugazhenthi, S., 2003. Cytokine-mediated down-regulation of the transcription factor cAMP-response element-binding protein in pancreatic B-cells. Journal of Biological Chemistry 278 (25), 23055–23065.

James, E.R., Green, D.R., 2004. Manipulation of apoptosis in the host-parasite interaction. Trends In Parasitology 20 (6), 280–287.

Kim, Y.M., Kim, T.H., Seol, D.W., Talanian, R.V., Billiar, T.R., 1998. Nitric oxide suppression of apoptosis occurs in association with an inhibition of Bcl-2 cleavage and cytochrome c release. Journal of Biological Chemistry 273, 31437–31441.

Kuwana, T., Bouchier-Hayes, L., Chipuk, J.E., Bonzon, C., Sullivan, B.A., Green, D.R., Newmeyer, D.D., 2005. BH3 domains of BH3-only proteins differentially regulate Bax-mediated mitochondrial membrane permeabilization both directly and indirectly. Molecular Cell 17, 525–535.

Law, P.T.W., Wong, C.-H., Au, T.C.C., Chuck, C.-P., Kong, S.-K., Chan, P.K.S., To, K.-F., Lo, A.W.I., Chan, J.Y.W., Suen, Y.-K., Chan, H.Y.E., Fung, K.-P., Waye, M.M.Y., Sung, J.J.Y., Lo, Y.M.D., Tsui, S.K.W., 2005. The 3a protein of severe acute respiratory syndrome-associated coronavirus induces apoptosis in Vero E6 cells. Journal of General Virology 86, 1921–1930.

Li, H., Zhu, H., Xu, C.-J., Yuan, J., 1998. Cleavage of BID by caspase 8 mediates the mitochondrial damage in the Fas pathway of apoptosis. Cell 94, 491–501.

Letai, A., Bassik, M.C., Walensky, L.D., Sorcinelli, M.D., Weiler, S., Korsmeyer, S.J., 2002. Distinct BH3 domains either sensitize or activate mitochondrial apoptosis, serving as prototype cancer therapeutics. Cancer Cell 2, 183–192.

Luo, X., Buhihardjo, I., Zou, H., Slaughter, C., Wang, X., 1998. Bid, a Bcl2 interacting protein mediates cytochrome c release from mitochondria in response to activation of cell surface death receptors. Cell 94, 481–490.

Liu, Y., Storm, D.R., 1989. Dephosphorylation of neuromodulin by calcineurin. Journal of Biological Chemistry 264 (22), 12800–12804.

Nicholson, D.W., 1999. Caspase structure, proteolytic substrates, and function during apoptotic cell death. Cell Death and Differentiation 6, 1028–1042.

Nechushtan, A., Smith, C.L., Lamensdorf, I., Yoon, S.-H., Youle, R.J., 2001. Bax and Bak coalesce into novel mitochondria-associated clusters during apoptosis. Journal of Cell Biology 153 (6), 1265–1276.

Nicholson, K.M., Anderson, N.G., 2002. The protein kinase B/Akt signalling pathway in human malignancy. Cellular Signalling 14, 381–395.

Oltvai, Z.N., Milliman, C.L., Korsmeyer, S.J., 1993. Bcl-2 heterodimerizes in vivo with a conserved homolog, Bax, that accelerates programmed cell death. Cell 74, 609–619.

Obata, T., Yaffe, M.B., Leparc, G.G., Piro, E.T., Maegawa, H., Kashiwagi, A., Kikkawa, R., Cantley, L.C., 2000. Peptide and protein library screening defines optimal substrate motifs for AKT/PKB. Journal of Biological Chemistry 275 (46), 36108–36115.

Peso, L.D., Gonzalez-Garcia, M., Page, C., Herrera, R., Nunez, G., 1997. Interleukin-3-induced phosphorylation of BAD through the protein kinase Akt. Science 278, 687–689.

Rehm, M., Huber, H.J., Dussman, H., Prehn, J.H., 2006. Systems analysis of effector caspase activation and its control by X-linked inhibitor of apoptosis protein. Embo Journal 25, 4338–4349.

Shibasaki, F., Kondo, E., Akagi, T., McKeon, F., 1997. Suppression of signaling through transcription factor NF-AT by interactions between calcineurin and Bcl-2. Nature 386, 728–731.

Shinoad, S., Schindler, C.K., Quan-Lan, J., Saugstad, J.A., Taki, W., Simon, R.P., Henshall, D.C., 2003. Interaction of 14-3-3 with Bid during seizure-induced neuronal death. Journal of Neurochemistry 86, 460–469.

Saito, A., Hayashi, T., Okuno, S., Ferrand-Drake, M., Chan, P.H., 2003. Overexpression of copper/zinc superoxide dismutase in transgenic mice protects against neuronal cell death after transient focal ischemia by blocking activation of the Bad cell death signaling pathway. Journal of Neuroscience 23 (5), 1710–1718.

Saito, S., Hiroi, Y., Zou, Y., Aikawa, R., Toko, H., Shibasaki, F., Yazaki, Y., Nagai, R., Komuro, I., 2000. β-adrenergic pathway induces apoptosis through calcineurin activation in cardiac myocytes. Journal of Biological Chemistry 275 (44), 34528–34533.

Springer, J.E., Azbill, R.D., Nottingham, S.A., Kennedy, S.E., 2000. Calcineurin-mediated Bad dephosphorylation activates the caspase-3 apoptotic cascade in traumatic spinal cord injury. Journal of Neuroscience 20 (19), 7246–7251.

Saito, M., Korsmeyer, S.J., Schlesinger, P.H., 2000. BAX-dependent transport of cytochrome c reconstituted in pure liposomes. Nature Cell Biology 2, 553–555.

Strasser, A., Huang, D.C., Vaux, D.L., 1997. Biochimica et Biophysica Acta 1333, 151–178.

Sedlak, T.W., Oltvai, Z.N., Yang, E., Wang, K., Boise, L.H., Thompson, C.B., Korsmeyer, S.J., 1995. Multiple Bcl-2 family members demonstrate selective dimerizations with Bax. Proceedings of the National Academy of Sciences 92, 7834–7838.

Spencer, S.L., Gaudet, S., Albeck, J.G., Burke, J.M., Sorger, P.K., 2009. Non-genetic origins of cell-to-cell variability in TRAIL-induced apoptosis. Nature Letters 459, 428–433.

Tan, Y., Ruan, H., Demeter, M.R., Comb, M.J., 1999. p90RSK blocks Bad-mediated cell death via a protein kinase C-dependent pathway. Journal of Biological Chemistry 274 (49), 34859–34867.

Valentijn, A.J., Metcalfe, A.D., Kott, J., Streuli, C.H., Gilmore, A.P., 2003. Spatial and temporal changes in Bax subcellular localization during anoikis. Journal of Cell Biology 162, 599–612.

Won, J., Kim, D.Y., La, M., Kim, D., Meadows, G.G., Joe, C.O., 2002. Cleavage of 14-3-3 protein by caspase-3 facilitates Bad interaction with Bcl-x(L) during apoptosis. Journal of Biological Chemistry 278 (21), 19347–19351.

Wei, M.C., Lindsten, T., Mootha, V.K., Weiler, S., Gross, A., Ashiya, M., Thompson, C.B., Korsmeyer, S.J., 2000. tBid, a membrane-targeted death ligand, oligomerizes BAK to release cytochrome c. Genes and Development 14, 2060–2071.

Wang, K., Yin, X.-M., Chao, D.T., Milliman, C.L., Korsmeyer, S.J., 1996. BID: a novel BH3 domain-only death agonist. Genes and Development 10, 2859–2869.

Wang, H.-G., Pathan, N., Ethell, I.M., Krajewski, S., Yamaguchi, Y., Shibasaki, F., McKeon, F., Bobo, T, Franke, T.F., Reed, J.C., 1999. Ca^{2+}-induced apoptosis through calcineurin dephosphorylation of BAD. Science 284, 339–343.

Wolff, D.J., Sved, D.W., 1985. The divalent cation dependence of bovine brain calmodulin-dependent phosphatase. Journal of Biological Chemistry 260 (7), 4195–4202.

Yi, X., Yin, X.-M., Dong, Z., 2003. Inhibition of Bid-induced apoptosis by Bcl-2. Journal of Biological Chemistry 278 (19), 16992–16999.

Yang, E., Zha, J., Jockel, J., Boise, L.H., Thompson, C.B., Korsmeyer, S.J., 1995. Bad, a heterodimeric partner for Bcl-xL and Bcl-2, displaces Bax and promotes cell death. Cell 80, 285–291.

Yin, X.M., Oltvai, Z.N., Korsmeyer, S.J., 1994. BH1 and BH2 domains of Bcl-2 are required for hinhibition of apoptosis and heterodimerization with Bax. Nature 369, 321–323.

Yaffe, M.B., Rittinger, K., Volinia, S., Caron, P.R., Aitken, A., Leffers, H., Gamblin, S.J., Smerdon, S.J., Cantley, L.C., 1997. The structural basis for 14-3-3: phosphopeptide binding specificity. Cell 91, 961–971.

Zhou, X.-M., Liu, Y., Payne, G., Lutz, R.J., Chittenden, T., 2000. Growth factors inactivate the cell death promoter BAD by phosphorylation of its BH3 domain on Ser155. Journal of Biological Chemistry 275 (32), 25046–25051.

Zha, J., Harada, H., Yang, E., Jockel, J., Korsmeyer, S.J., 1996. Serine phosphorylation of death agonist BAD in response to survival factor results in binding to 14-3-3 not BCL-XL. Cell 87, 619–628.

Zhou, G.-L., Zhuo, Y., King, C.C., Fryer, B.H., Bokoch, G.M., Field, J., 2002. Akt phosphorylation of Serine 21 on Pak1 modulates Nck binding and cell migration. Molecular and Cellular Biology 23 (22), 8058–8069.